PHYSICAL REVIEW B **83**, 121407(R) (2011)

Triple junction segregation in nanocrystalline multilayers

P. Stender,* Z. Balogh, and G. Schmitz
Institute of Material Physics, University of Muenster, Germany
(Received 25 January 2011; published 22 March 2011)

Triple junctions (TJ's), topologically required linear defects of grain boundary structure, are suggested to control the behavior of nanocrystalline material. However, measurements of their properties are rare. With atom probe tomography, reliable analysis of singular features of the grain boundary structure becomes possible. We report microscopic measurements of segregation along individual TJ's in Fe/Cr. By segregation to TJ's nanometric tubular objects of distinct properties are formed. The determined segregation enthalpy of 0.076 eV indicates that TJ's provide considerable free volume similar to free surfaces.

DOI: 10.1103/PhysRevB.83.121407 PACS number(s): 68.37.Vj, 64.75.Jk, 61.72.Mm

Nanostructured materials display unique features and have attracted great interest.[1] Improved hardness or plasticity, soft or hard magnetic properties, wetting, and absorption phenomena have made them a bearer of hope for the solution of a wide range of problems in material science, engineering, and medicine. Since the volume fraction of grain boundaries (GB's) increases with decreasing grain size, it is important to gain a full understanding of GB's.[2,3] Even more, substructures of the GB morphology, in particular triple junctions (TJ's), that is, the line-shaped topological defect at which three boundaries merge, will presumably control material properties, if grain size scales down to the nanometer range. Particular physical properties of TJ's are proposed in theoretical work[4] and computer simulation[5] while experimental evidence is rare. TJ's may provide paths of increased diffusivity,[3] preferential sites of chemical attacks, wetting and segregation, or nucleation of new grains.[6] The mobility of TJ's is demonstrated to play a crucial role in grain growth.[7] Furthermore, they could be a source of pinholes.[8]

Measuring properties of individual TJ's is an experimental challenge, especially in nanocrystalline microstructures. TJ's represent line-shaped defects with diameters close to atomic distances. They are embedded in the complex 3D morphology of adjacent grains. In this situation, electron microscopy suffers from projection artifacts. Reported attempts[6] of measuring segregation by electron microscopy eventually misinterpreted wetting by low melting metals.[9] Only indirect experimental evidence stems from macroscopic observations (measurement of mechanical, electronic, or magnetic behavior and tracer diffusion or surface accumulation).

Direct chemical analysis of embedded line-shaped objects requires microscopy that provides subnanometer resolution in all three dimensions. Atom probe tomography has proven to be an efficient tool of local three-dimensional (3D) analysis.[10] In particular, successful investigations of Cottrell clouds at dislocations[11–13] have pointed out its unique capability. In recent years, the total volume of analysis of respective instruments have been significantly increased so that even rare defects can be analyzed with sufficient statistical significance.[14] In this work, we present experiments on multilayer model structures of Fe/Cr, in particular on the distribution of Cr in nanocrystalline Fe layers. Depositing metallic multilayers by ion beam sputtering produces a nanocrystalline microstructures. Beside its model character, Fe-Cr is of particular importance in a broad range of applications.

In 1988, Grünberg and Fert discoverd the giant magnetoresistance (GMR) effect using Fe/Cr/Fe trilayers[15] or multilayer stacks $\{Fe/Cr\}_n$.[16] The magnitude of the GMR amplitude depends on the integrity of very thin layers. Even slight disturbances such as, for example, pinholes induced by segregation along TJ, may already degrade the effect amplitude.

Recently, particular efforts have been made to understand the properties of this important metallic system using computer simulations with regard to surface segregation,[17] interstitials,[18] magnetism and thermodynamics,[19] and electronic influences on the stability.[20] Therefore, the quantitative data presented in the following will motivate further theoretical work in the near future.

Atom probe tomography requires a needle-shaped sample with a radius of curvature of 50 to 100 nm to produce field strengths of about 30 V/nm at the apex. Applying high-voltage pulses, atoms of the specimen are field-evaporated and chemically identified by time-of-flight mass spectrometry. Using a position-sensitive detector system to register impact positions of the incoming atoms, individual atoms within the sample are localized with subnanometer accuracy. A 3D volume reconstruction of the eroded material is obtained by postprocessing of the data.

In previous studies, nanocrystalline thin films for atom probe analysis were deposited directly upon field-developed tungsten tips to obtain the required sample geometry.[21] With this technique, deposited layer stacks get curved and cannot directly compared to planar GMR sensors. Therefore, a more complex specimen preparation[22] was accepted to obtain flat interfaces: A custom-made UHV ion beam sputtering system, dedicated to the coating of tip-shaped substrates, was used to deposit a buffer layer of 100-nm chromium on blunted tungsten substrate posts with a flat top surface of 1 to 2 μm diameter, followed by the desired $\{Fe_{10nm}Cr_{12nm}\}_{25}$ multilayer. Finally, a protective cap layer of 50-nm chromium was deposited. This final layer acts as a protective coating against oxidation and irradiation damage in subsequent preparation steps. After deposition, these samples were annealed in the temperature range from 573 to 1073 K for 30 minutes in a vacuum furnace with a residual gas pressure of $<1 \times 10^{-8}$ mbar. After thermal treatment, they were sharpened by annular milling[23] to a radius of curvature smaller than 100 nm.

Analysis was carried out using the wide angle tomographic atom probe (WATAP) constructed at the Institute of Material

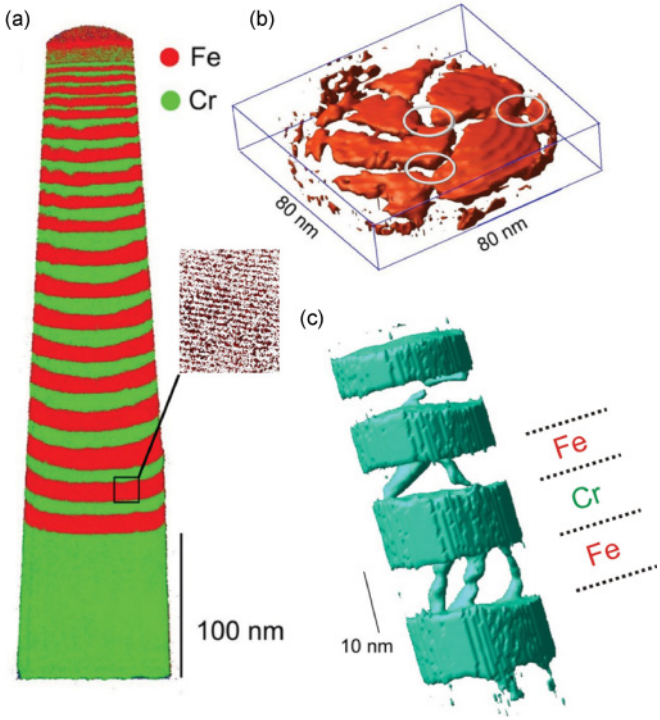

FIG. 1. (Color online) (a) Atomic reconstruction of the as-prepared sample (>100 million atoms). (b) Isosurface plot (97 at.% Fe) of iron layer (annealed at 873 K) discovers the grain morphology. (c) Isoconcentration surface (40 at.% Cr) demonstrates line-shaped segregation zones bridging the Fe layers.

Physics, University of Münster, Germany.[24] The instrument is equipped with a 120-mm delay line detector. It offers a flight length of 150 mm and a numerical aperture of ±35°. The typical lateral width of investigated volumes amounts to 100 nm. Specimens were evaporated at a pulse rate of 20 kHz, a pulse fraction $U_{\text{pulse}}/U_{\text{DC}} = 20\%$, and a temperature of 35 K.

Energy-filtered TEM and FIM demonstrate a well-defined multilayer geometry in as-deposited samples.[22] Columnar grains with a lateral diameter of about 20 nm spread across several consecutive layers.[25] The tomographic reconstruction of the atom probe measurement [Fig. 1(a)] confirms this layer geometry. By local chemical analysis (even lattice planes are resolved in reconstructions, see small inset), the chemical width of the layer interfaces is determined to be only 0.4 nm. In atom probe data, GB's are frequently distinguished by locally reduced atomic density. In addition, they are marked by a small but measurable segregation of the minority component after annealing. Therefore, plotting respective isosurfaces of density or composition, the grain morphology is directly imaged, as exemplified in [Fig. 1(b)]. Owing to the large field of view, several grains are included in the analyzed volume of a single measurement. Thus, the position of TJ's is clearly identified, as marked by circles in the figure.

By annealing, chromium starts diffusing into the bulk of the iron layers while the atomic mobility inside Cr is too low to allow significant mixing. Since the required diffusion length amounts to only a few nanometers, the Cr concentration inside Fe reaches the solubility limit in contact to pure Cr already after only 30 min of annealing at 773 K or higher temperatures. As expected, this solubility increases steadily with temperature (see the inset of Fig. 3; see the table in Ref. 25 for more details). After 30 min annealing at 1073 K, individual Fe and Cr layers are no more distinguished. Instead, the average concentration of the multilayer of about 60 at.% Cr is established throughout the volume by complete mixing. In all investigated stages, formation of the complex σ phase is suppressed by kinetic limitation.

Striking and most remarkable in the present context is the formation of pipelike segregation zones that cross the layers as demonstrated by the isoconcentration plot in Fig. 1(c). Inside the Fe layers, the concentration within these pipes significantly exceeds the Cr content in surrounding bulk and GB's. By comparison with the grain morphology [Fig. 1(b)], these segregation lines are unambiguously correlated to TJ's between merging GB's. Two types of TJ's can be distinguished. The first represents lines that bridge only a single layer as shown in Fig. 1(c). TJ's of the second type cross even several consecutive layers of the multilayer stack [Fig. 2(a)], which is naturally explained by the columnar microstructure. Similar segregation phenomena are also noticed inside the Cr layers.

With increasing annealing temperature, triple lines of the second type tend to assume a remarkably straight geometry and exhibit high concentrations of chromium inside the Fe layers. For this reason, only TJ's of this kind are evaluated in the following. In Fig. 2(b), a two-dimensional composition map is shown, determined perpendicular to a TJ within the Fe layer. The lateral dimension of the Cr-enriched line amounts to 1.5–2 nm in diameter. For further evaluation, the line is divided into consecutive slices, each 1 nm in thickness. A composition

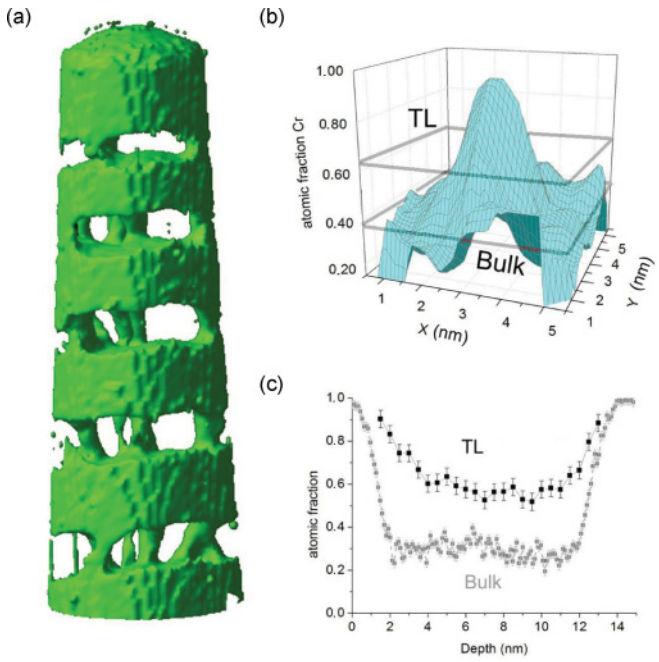

FIG. 2. (Color online) Sample after 30 min annealing at 973 K. (a) Isoconcentration surface (60 at.% Cr) revealing triple junctions spreading across several consecutive layers. (b) 2D composition map perpendicular to a line-shaped segregation zone. (c) Composition profiles along TJ and through bulk of the Fe film.

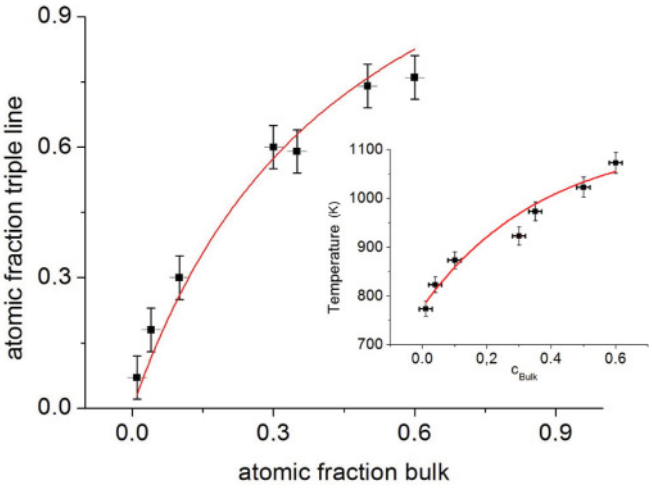

FIG. 3. (Color online) Local composition of triple line vs composition of bulk Fe layer. Solid line was calculated using Eq. (1). Inset presents Cr solubility of thin Fe layers in equilibrium to pure Cr.

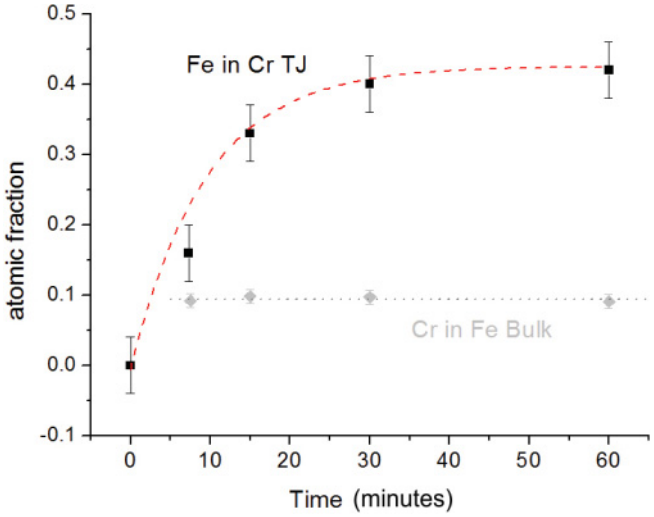

FIG. 4. (Color online) Time evolution of the concentrations at 873 K. After 30 min of annealing the Fe concentration in the Cr TJ's reach a saturation. The Cr content in the Fe layer is independent of the annealing time and reasonably close to the equilibrium concentration predicted by the phase diagrams.

map similar to that in Fig. 2(b) is calculated for each slice. Concentration floor of the bulk and excess of the line are determined as indicated in Fig. 2(b) and from these, the average concentration of the TJ is determined. The consecutive series of these averages represent a composition profile along an individual line, as presented in Fig. 2(c), in direct comparison to a similar profile through the bulk aside the line. In the middle of the layer, the TJ profile reveal an approximate plateau. Averaging the plateau levels of three to eight individual TJ's at given temperature, the segregation level at the TJ is evaluated (Fig. 3).

The described procedure yields a consistent dependence on temperature as is demonstrated by Fig. 3. It is important to clarify whether the data of Fig. 3 represent equilibrium values. Therefore an isothermal annealing sequence was carried out at 873 K. Inside the Fe layers, volume diffusivity is sufficient to establish solubility limit in the bulk even after short annealing temperatures. After 7.5 minutes the equilibrium value is already established, as demonstrated by Cr in Fe bulk values in Fig. 4. Bulk diffusion processes are by order of magnitude slower than grain boundary processes and it is reasonable to assume an even faster transport inside the TJ's.

By contrast, the diffusivity of Fe inside the Cr layers is a few orders of magnitude slower in comparison to the diffusion of Cr inside Fe layers. Up to 1023 K, no iron is detected within the Cr layers, except in TJ's. Nevertheless, we can demonstrate by isothermal annealing treatment that in spite of this slower kinetics, the concentration inside the TJ's saturates at a constant level after about 30 min annealing (see Fig. 4). These observations demonstrate first hand a faster transport along TJ's than along GB's or bulk. Furthermore, they confirm that our annealing treatments are certainly sufficient to establish equilibrium inside the TL's, especially inside the Fe layers revealing the faster transport. We therefore conclude that the measurements presented in Fig. 3 represent equilibrium data.

The following discussion focusses to the properties of TJ's in Fe. The segregation factor in dilute limit is determined to a value about $s = 3$. As demonstrated by the solid line, compositions are reasonably described by the Langmuir-McLean theory first introduced for surface segregation:[26]

$$\frac{c_{\mathrm{TJ}}}{1 - c_{\mathrm{TJ}}} = \frac{c_{\mathrm{bulk}}}{1 - c_{\mathrm{bulk}}} \cdot \exp\left\{\frac{H_{\mathrm{seg}}}{k_B T}\right\}. \qquad (1)$$

By fitting, the segregation enthalpy of the TJ is determined to (0.076 ± 0.002) eV. We can compare that to the 0.159 eV segregation enthalpy of Cr at a free surface of Fe.[27] In the same paper a grain boundary segregation measurement is also reported; using those values, a grain boundary segregation enthalpy of 0.030 eV can be calculated. Thus, the microscopically determined value of the TJ nicely fits between the surface and the GB case.

Contemporary theories of segregation[28–30] describe the segregation enthalpy by a complex combination of elastic, chemical, and surface tension related driving forces often in multilayered models. Unfortunately the rather low value of the segregation enthalpy in the Fe-Cr system does not allow us to clearly separate those terms without detailed molecular statics calculation based on first principle interaction potentials. However, it is generally true for all of those driving forces that more free volume/broken bonds result in a higher segregation enthalpy. Obviously, the geometric structure of the triple line represents significant excess volume so that atomic binding gets in between the free surface and normal grain boundary.

The unique capability of three-dimensional analysis with single-atom sensitivity by atom probe tomography allowed observation and characterization of individual triple lines in nanocrystalline films. Distinguished segregation of chromium to triple junctions in iron, different from wetting, was clearly demonstrated. The respective segregation amplitude exceeds that of neighbored high angle GB's significantly, which emphasizes distinguished physical properties of triple junctions.

The presented experiments document that singular features of the grain boundary structure can be measured accurately by 3D atom probe tomography with statistical significance.

It is remarkable that the proven enrichment along the TJ's reaches several tens of atomic percent. In contrast to usual tracer experiments, segregation is not measured in the dilute limit but to technical important levels. Thus, nanometric, tubelike objects of distinct physical properties are formed by segregation. It will be an attractive topic of future research to determine, for example, the magnetic properties of these tubes.

Since segregation to TJ is more pronounced than that to ordinary grain boundaries, the former may act as centers of early pinhole formation and thus represent the decisive objects to initialize the fragmentation of the multilayer structure. Indeed, in further experiments with similar multilayers, we demonstrated that the onset temperature of degradation of the GMR amplitude matches closely to the onset temperature of TJ segregation.[31] On the other hand, pronounced segregation will certainly decrease the specific energy of TJs and hinder their migration by solute drag. Both factors may increase the stability of nanocrystalline microstructures with respect to grain growth and recrystallization.

Financial support by the German Science foundation (SCHM 1182/9) is gratefully acknowledged.

*patricks@uni-muenster.de

[1]H. Gleiter, Acta Mater. **48**, 1 (2000).
[2]R. A. Andrievski, Mater. Sci. Forum **494**, 113 (2005).
[3]Y. Chen and C. A. Schuh, Scripta Mater. **57**, 253 (2007).
[4]A. H. King, Interface Sci. **7**, 251 (1999).
[5]T. Frolov and Y. Mishin, Phys. Rev. B **79**, 174110 (2009).
[6]K. M. Yin, A. H. King, T. E. Hsieh, F. R. Chen, J. J. Kai, and L. Chang, Microsc. Microanal. **3**, 417 (1997).
[7]F. Barrales Mora, V. Mohles, L. S. Shvindlerman, and G. Gottstein, Acta Mater. **56**, 1151 (2008).
[8]F. Y. Genin, W. W. Mullins, and P. Wynblatt, Acta Metall. Mater. **40**, 3239 (1992).
[9]B. Straumal, B. Bokstein, A. Straumal, and A. Petelin, JETP Lett. **88**, 537 (2008).
[10]D. J. Larson, A. Cerezo, J. Juraszek, K. Hono, and G. Schmitz, MRS Bull. **34**, 732 (2009).
[11]M. K. Miller, J. Mater. Sci. **41**, 7808 (2006).
[12]D. Blavette, E. Cadel, A. Fraczkiewicz, and A. Menand, Science **286**, 2317 (1999).
[13]J. Wilde, A. Cerezo, and G. D. W. Smith, Scripta Mater. **43**, 39 (2000).
[14]T. F. Kelly and M. K. Miller, Rev. Sci. Instrum. **78**, 031101 (2007).
[15]G. Binasch, P. Grünberg, F. Saurenbach, and W. Zinn, Phys. Rev. B. **39**, 4828 (1989).
[16]M. N. Baibich, J. M. Broto, A. Fert, F. Nguyen van Dau, F. Petroff, P. Etienne, G. Creuzet, A. Friederich, and J. Chazelas, Phys. Rev. Lett. **61**, 2472 (1988).
[17]A. Kiejna and E. Wachowicz, Phys. Rev. B **78**, 113403 (2008).
[18]T. P. C. Klaver, P. Olsson, and M. W. Finnis, Phys. Rev. B **76**, 214110 (2007).
[19]T. P. C. Klaver, R. Drautz, and M. W. Finnis, Phys. Rev. B **74**, 094435 (2006).
[20]P. Olsson, I. A. Abrikosov, and J. Wallenius, Phys. Rev. B **73**, 104416 (2006).
[21]J. Schleiwies, G. Schmitz, S. Heitmann, and A. Hütten, Appl. Phys. Lett. **78**, 3439 (2001).
[22]P. Stender, T. Heil, H. Kohl, and G. Schmitz, Ultramicroscopy **109**, 612 (2009).
[23]D. J. Larson, A. K. Petford-Long, Y. Q. Ma, and A. Cerezo, Acta Mater. **52**, 2847 (2004).
[24]P. Stender, C. Oberdorfer, M. Artmeier, P. Pelka, F. Spaleck, and G. Schmitz, Ultramicroscopy **107**, 726 (2007).
[25]See supplemental material at [http://link.aps.org/supplemental/10.1103/PhysRevB.83.121407] for the FIM and TEM images.
[26]D. McLean, *Grain Boundaries in Metals* (Oxford University Press, London, 1957).
[27]Y. S. Ng and T. T. Tsong, Surf. Sci. **78**, 419 (1978).
[28]J. Creuze, I. Braems, F. Berthier, C. Mottet, G. Tréglia, and B. Legrand, Phys. Rev. B **78**, 075413 (2008).
[29]F. Berthier, B. Legrand, and G. Tréglia, Acta Mater. **47**, 2705 (1999).
[30]D. L. Beke, C. Cserháti, Z. Erdélyi, and I. A. Szabó, in *Segregation in Nanostructures*, edited by H. S. Nalwa (American Scientific Publishers, Valencia, CA, 2003), Chap. 7.
[31]P. Stender, Ph.D. thesis (University of Münster, Münster, Germany, 2010).